R-05-10

Representation of an open repository in groundwater flow models

Scott Painter, Alexander Sun
Center for Nuclear Waste Regulatory Analyses
Southwest Research Institute®

August 2005

Svensk Kärnbränslehantering AB
Swedish Nuclear Fuel
and Waste Management Co
Box 5864
SE-102 40 Stockholm Sweden
Tel 08-459 84 00
+46 8 459 84 00
Fax 08-661 57 19
+46 8 661 57 19

ISSN 1402-3091
SKB Rapport R-05-10

Representation of an open repository in groundwater flow models

Scott Painter, Alexander Sun
Center for Nuclear Waste Regulatory Analyses
Southwest Research Institute®

August 2005

Contents

1 Background

The effect of repository tunnels on groundwater flow has been identified as a potential issue for the nuclear waste repository being considered by SKB for a fractured granite formation in Sweden. In particular, the following pre-closure and post-closure processes have been identified as being important:

- inflows into open tunnels as functions of estimated grouting efficiencies,
- drawdown of the water table in the vicinity of the repository,
- upconing of saline water,
- "turnover" of surface water in the upper bedrock, and
- resaturation of backfilled tunnels following repository closure.

In the current groundwater models, open tunnels prior to repository closure are represented within far-field saturated flow models using a fixed pressure condition at those nodes that coincide with tunnels. Groundwater flow after the tunnels have been backfilled and closed is modeled by using the calculated pre-closure condition as the initial condition in a transient saturated groundwater model. These representations of repository tunnels are approximate because many of the processes that affect the groundwater dynamics near the tunnels are unique to partially saturated porous media or are fully two-phase (gas, liquid) phenomena that are not represented in saturated groundwater models. The formation of a two-phase region in the immediate vicinity of tunnels may reduce the relative permeability to liquid flow, thereby reducing inflows into the tunnels. Forced ventilation within the tunnels may remove moisture from the host rock, further amplifying this effect. The potential role of a two-phase region in reducing tunnel inflows has been recognized previously in the SKB program – a "skin factor" is sometimes applied to reduce inflows, for example – but the magnitude of this effect has not been quantified.

The representation of repository tunnels within groundwater models is addressed in this report. The primary focus is on far-field flow that is modeled with a continuum porous medium approximation. Of particular interest are the consequences of the tunnel representation on the transient response of the groundwater system to repository operations and repository closure, as well as modeling issues such as how the water-table free surface and the coupling to near-surface hydrogeology should be handled. The overall objectives are to understand the consequences of current representations and to identify appropriate approximations for representing open tunnels in future groundwater modeling studies.

2 Tunnel representation in far-field flow models

2.1 Approach

A series of numerical simulations was used to investigate the effect of various tunnel representations on water-table drawdown in the vicinity of a hypothetical repository in the saturated zone. Flow into the open repository was first represented using a fully two-phase flow model. This representation was then simplified by neglecting gas movement but still retaining the unsaturated/saturated representation (Richards equation representation). In the final approximation, unsaturated-zone processes were neglected. That is, an unconfined-aquifer approximation was used, wherein saturated flow is represented below a moving water table and flow is neglected above this free surface. The latter approximation is similar to the unconfined mode of MODFLOW /Harbaugh et al. 2000/, wherein unsaturated grid cells are simply removed from the calculations, as well as more sophisticated computer codes that explicitly track a moving boundary corresponding to the water table.

2.2 Mathematical model

The METRA module of the MULTIFLO system /Painter and Seth, 2003/ was used in the numerical experiments. METRA models two-phase (gas, liquid), two-component (air, H_2O) flow and energy transport in partially saturated porous/fractured media. For this study, a single continuum porous medium representation was used wherein flow in fractures is represented by an equivalent continuum, and flow and storage in the rock matrix is neglected.

METRA solves conservation equations for H_2O, air, and energy. The conservation equation for the H_2O (w) component is given by

$$\frac{\partial}{\partial t}\left[\phi\left(s_l n_l X_l^w + s_g n_g X_g^w\right)\right] + \nabla\cdot\left(q_l n_l X_l^w + q_g n_g X_g^w - D_g n_g \nabla X_g^w\right) = Q_w, \qquad (1)$$

where t denotes time, ϕ the porosity, Q_w the H_2O source, and D_g the gas diffusion coefficient. For the phase-dependent quantities, the subscripts l and g denote liquid or gas, respectively: s_l (s_g) is the phase saturation, n_l (n_g) the molar density, and X_l^w (X_g^w) the mole fraction of H_2O in liquid (gas). The corresponding equation for the air (α) component is

$$\frac{\partial}{\partial t}\left[\phi\left(s_l n_l X_l^a + s_g n_g X_g^a\right)\right] + \nabla\cdot\left(q_l n_l X_l^a + q_g n_g X_g^a - D_g n_g \nabla X_g^a\right) = Q_a. \qquad (2)$$

The mole fractions and phase saturations satisfy the following relations:

$$X_l^w + X_l^a = 1, \quad X_g^w + X_g^a = 1 \text{ , and } s_l + s_g = 1. \qquad (3)$$

It is convenient to replace the water balance equation with an equation for total mass. Adding Equations (1) and (2) eliminates the diffusive terms and results in the following equation for total (air plus H_2O) mass:

$$\frac{\partial}{\partial t}\left[\phi\left(s_l n_l + s_g n_g\right)\right] + \nabla\cdot\left(q_l n_l + q_g n_g\right) = Q_w + Q_a \tag{4}$$

Equations 1 and 4 form the basis for the METRA simulations summarized in this report. METRA also solves a coupled energy balance equation. For the present application, the system is modeled as isothermal and the energy balance is not relevant.

The Darcy fluxes for liquid, q_l, and gas, q_g, are defined by

$$q_l = -\frac{kk_l}{\mu_l}\nabla\left(P_l - \rho_l g z\right), \tag{5}$$

and

$$q_g = -\frac{kk_g}{\mu_g}\nabla\left(P_g - \rho_g g z\right), \tag{6}$$

where P_l (P_g) is pressure, μ_l (μ_g) viscosity, ρ_l (ρ_g) mass density, and k_l (k_g) relative permeability for liquid (gas) phases. The symbols z and g are the vertical coordinate and acceleration due to gravity, respectively. The symbol k without a subscript denotes absolute permeability. The liquid and gas pressures are related through the capillary pressure P_c:

$$P_l = P_g - P_c \tag{7}$$

Several additional constitutive relationships are required to close the system of equations. The most important ones are the relationship between the capillary pressure and saturation (characteristic curve), and the relationships between relative permeability and saturation. For the current work, the /van Genuchten, 1980/ model is used:

$$s_l^{\text{eff}} = \left[1 + \left(\alpha\left|P_c\right|\right)^m\right]^{-\lambda} \tag{8}$$

where s_l^{eff} is the effective or reduced liquid saturation defined by

$$s_l^{\text{eff}} = \frac{s_l - s_l^r}{1 - s_l^r} \tag{9}$$

where s_l^r is the residual saturation. The quantities α and λ are van Genuchten's fitting parameters, and $m = 1/(1-\lambda)$.

Relative permeability for the liquid phase is given by

$$k_l = \sqrt{s_l^{\text{eff}}}\left\{1 - \left[1 - \left(s_l^{\text{eff}}\right)^{1/\lambda}\right]^{\lambda}\right\}^2, \tag{10}$$

and for the gas phase by $k_g = 1 - k_l$.

The other major constitutive relationships are the equation-of-state for water and the various thermophysical properties of liquid water and water vapor. Accurate high-order curve fits or table lookups based on the IFC-67 /International Formulation Committee, 1967/ formulation are used for these relationships.

METRA does not have explicit options for the Richards approximation or the unconfined aquifer approximation. However, both can be modeled through appropriate choice of boundary conditions or property assignment. Gas flow can be suppressed by specification

of appropriate boundary conditions. Specifically, when capillary pressure is set to zero at the tunnel, then single-phase flow is maintained in the tunnel vicinity. With no imposed macroscopic gas pressure gradients to drive gas flow in the unsaturated zone, this combination of assumptions results in very little gas movement as in the Richards approximation. The unconfined aquifer model is implemented by also specifying very weak moisture retention properties for the medium so that a sharp interface between fully saturated and fully dry conditions is maintained.

2.3 Model configuration and scenario

The model configuration is shown in Figure 2-1. The repository is modeled as a set of eight concentric ring tunnels in the horizontal plane at a depth of 390 m. This configuration is not intended to be an accurate representation of an actual repository layout, which would likely be an array of linear horizontal tunnels. The model configuration allows the simulation to be done in cylindrical coordinates and two dimensions (radius and depth) as opposed to

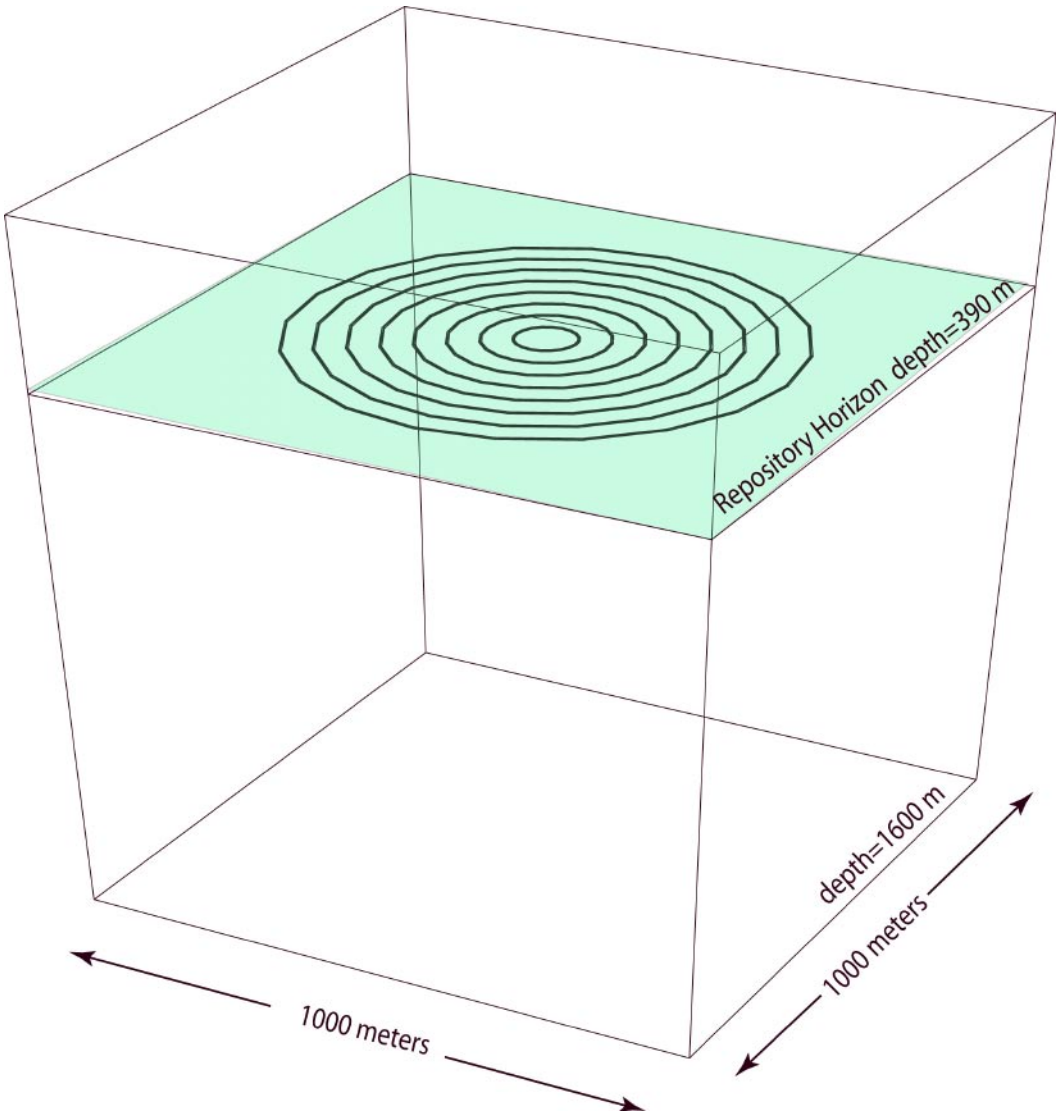

Figure 2-1. *Radial repository configuration considered in the far-field simulations. Eight concentric tunnels are used to represent the repository. The tunnels are labeled 1–8 starting from the innermost tunnel.*

three dimensions, while still capturing “edge effects” adequately. Specifically, water can flow into the repository footprint from all directions and must flow around the outer tunnels before reaching the inner tunnels. This radial configuration allows a better representation of drawdown near the center of the repository footprint as compared to a two-dimensional Cartesian representation. The repository footprint occupies about 40,000 m^2. Each tunnel has a square cross section with 5 m per side.

The model domain (Figure 2-2) extends from the ground surface to a depth of 1,500 m, and from the repository center to a distance of 8,000 m radially. No-flow boundary conditions are used for the bottom and r = 0 boundaries. A specified infiltration rate of 25 mm/year /Jaquet and Siegel, 2004; Walker et al. 1997/ is applied to the top boundary, and gas pressure at this boundary is held at one atmosphere. The outer boundary (r = 8,000 m) is assumed to be sufficiently distant from the repository so that hydrostatic conditions equal to the initial condition apply.

The model domain is divided into three hydrostratigraphic units. The hydrostratigraphy (see Figure 2-2), and the overall model configuration are similar to those used by /Jaquet and Siegel, 2004/ in modeling of the Beberg site.

The model grid is comprised of 175 cells vertically and 80 cells radially, for a total of 14,000 cells. The grid spacing is small near the tunnels and becomes coarser away from the tunnel locations. The model grid in the repository area is shown in Figure 2-3a. A detail close to the innermost tunnel is shown in Figure 2-3b.

The initial condition is hydrostatic with a water table depth of 15 m. The simulations are started by instantaneously lowering the pressure in the tunnel cells to 1 atmosphere.

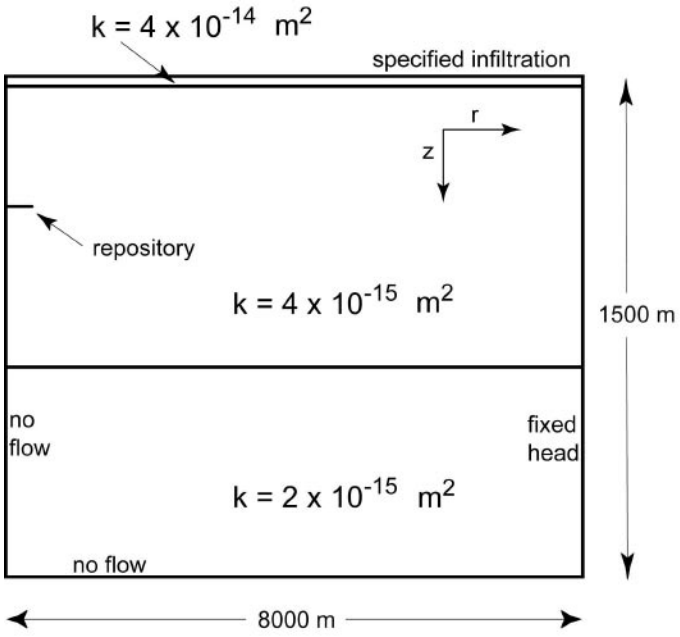

Figure 2-2. *Model domain in cylindrical coordinates showing the hydrostratigraphy and boundary conditions used in the far-field flow simulations.*

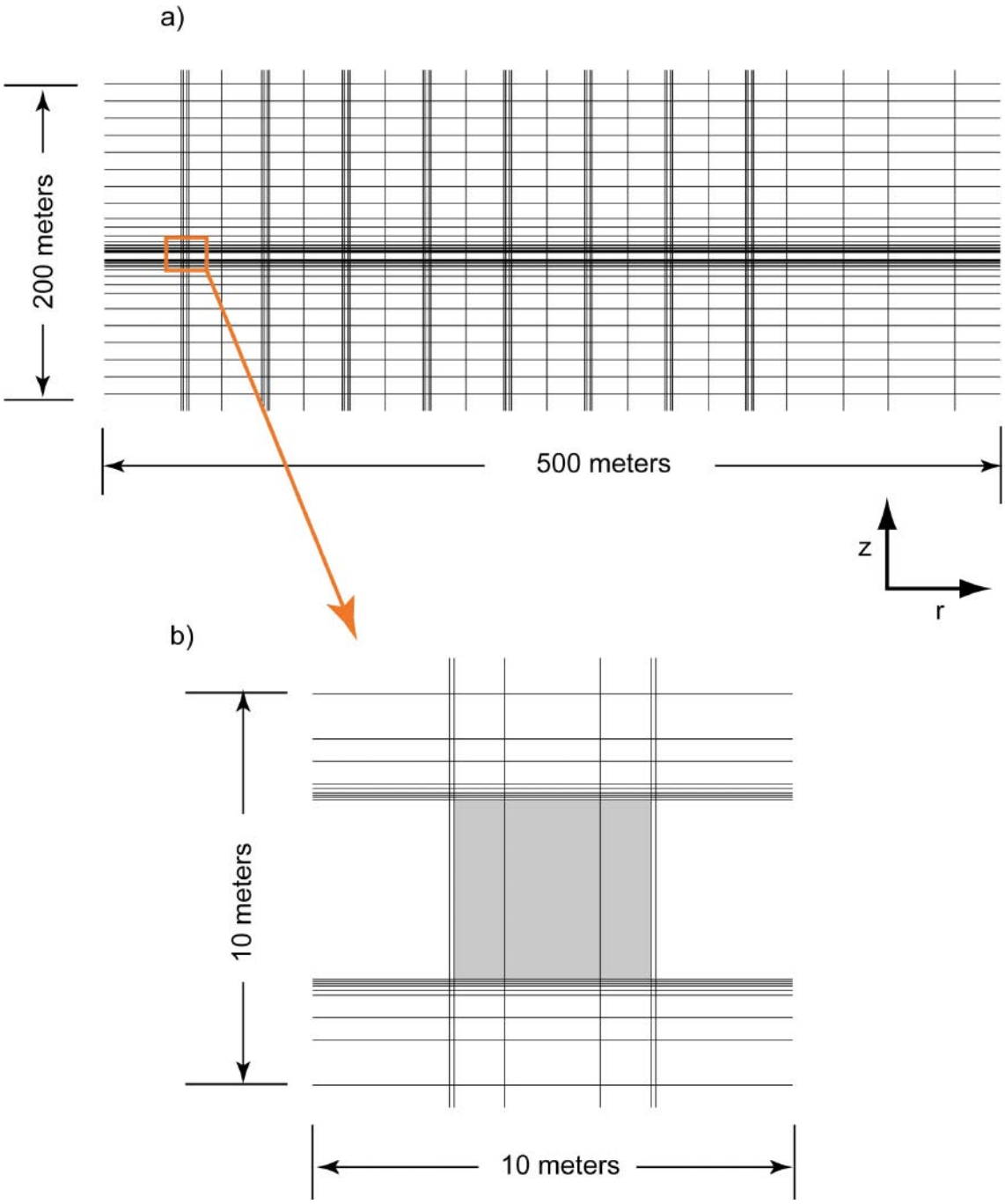

Figure 2-3. *Computational grid: (a) near the repository region, and (b) immediate vicinity of the innermost tunnel. The shaded area in (b) represents the interior of the tunnel.*

2.4 Model parameters for reference and variant cases

Parameters that must be specified for the model include permeability, porosity, and the van Genuchten parameters α and λ. Permeability values for the three hydrostratigraphic units are shown in Figure 2-2. Porosity is set to 0.02 for all units. These permeability values are consistent with those developed by /Jaquet and Siegel, 2004/ by upscaling stochastically generated discrete fracture networks. These permeability and porosity values are used for the reference case.

The van Genuchten parameters quantify the moisture retention properties of the medium. For the fractured granite formations under consideration, these parameters are highly uncertain. The best estimates are probably those of /Jarsjö et al. 2001/, who consider multiphase flow in a single fracture. They developed a theoretical model for the retention properties of a heterogeneous fracture and compared this model to the van Genuchten model. They show that a van Genuchten model with $\alpha = 8\times10^{-4}$ Pa^{-1} and $\lambda = 0.54$ can be used to describe the moisture retention properties of a heterogeneous fracture with geometric mean of aperture of about 50 μm. These values are used for the reference case. The relative permeability curve for the reference case is shown in Figure 2-4. However, it is noted that the van Genuchten parameters are uncertain because the /Jarsjö et al. 2001/ work focuses on a single heterogeneous fracture and is not clear how this might apply at the continuum scale for a network with many fractures of different sizes. The most reliable way to obtain characteristic curves for fracture networks that are applicable at the continuum scale is by inverse modeling of controlled infiltration experiments. This inverse modeling of experiments has not been done for the Swedish fractured granite formations.

The reference case uses the two-phase option. The initial dissolved air content is at equilibrium with one atmosphere. A capillary pressure (suction) of 1 MPa is applied to the tunnel nodes to simulate the drying effects of ventilation air.

The variants from the reference case are as follows:

Drain: In this simulation, the capillary suction is set equal to zero at the tunnel nodes, and other parameters are the same as the reference case. With this boundary condition, the pressure near the tunnels does not drop below the bubble point and flow remains single-phase. Flow above the water table may be two-phase, but as noted in the previous section, there are no imposed macroscopic gas pressure gradients to drive gas flow, and the gas is nearly a passive bystander in the simulation. This scenario is very similar to a simulation based on Richards equation.

Unconfined Aquifer: In this simulation, the tunnel boundary condition is the same as in the Drain simulation. In addition, the capillary pressure is set to zero for all cells for all values of liquid saturation. The result of this parameter assignment is a sharp interface between fully saturated cells and fully dry cells. This simulation is equivalent to the unconfined mode of MODFLOW and approximates a free-surface code.

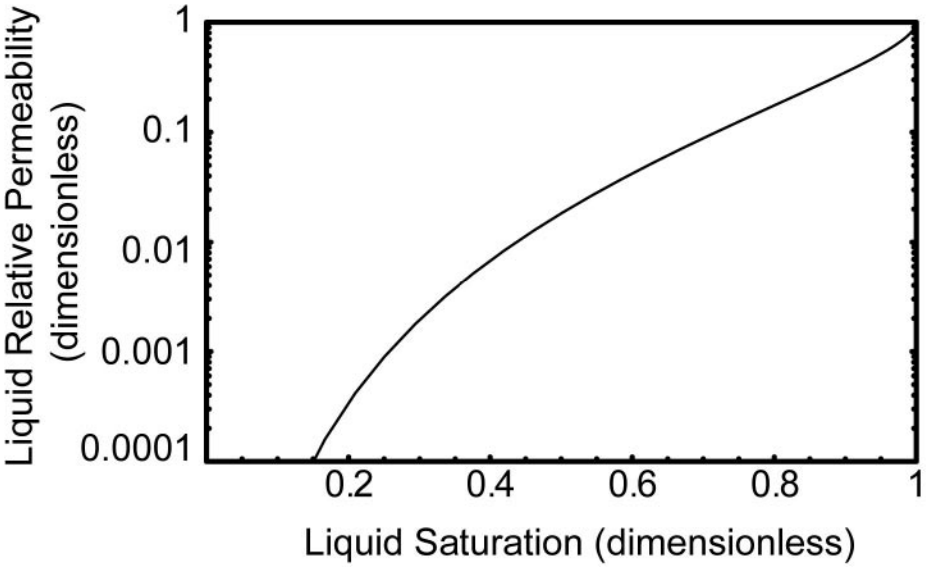

Figure 2-4. *Relative permeability curve for the reference case.*

Air: The initial dissolved air fraction is elevated by a factor of two relative to the reference case in this simulation. That is, the air bubble pressure is two atmospheres. Elevated air fractions have been observed in deep Swedish formations, indicating subsurface gas generation, possibly biological in origin /Jarsjö et al. 2001/. With the elevated bubble pressure, a larger two-phase flow region forms around the repository tunnels.

Weak Suction: The reference case uses a capillary suction of 1 MPa to simulate the effects of ventilation-induced drying. /Siegel et al. 2002/ uses a capillary suction of 5 MPa when studying similar processes in a repository situated in a clay formation, but provide no technical basis for this assumption. At present, little independent information exists on the appropriate value for the imposed capillary suction. Although models developed to study the drying effects of ventilation in the potential repository at Yucca Mountain are available and could be applied to this problem, an appropriate first step is to simply test sensitivity to the imposed capillary suction. In the Weak Suction case, the capillary pressure at the tunnel cells is set to 2×10^5 Pa, a factor of five lower than in the reference case.

Strong Suction: In this simulation, the capillary suction at the tunnel cells is set to 5 MPa to simulate more ventilation-induced drying than the reference case.

Smeared Repository: The repository is represented as a disk with radius of 360 m (instead of discrete concentric ring tunnels) in this simulation.

Increased Permeability: The permeability in all units is increased by 100% relative to the reference case.

Decreased Permeability: The permeability in all units is decreased by 50% relative to the reference case.

Increased Infiltration: The infiltration is increased by 100% relative to the reference case.

Decreased Infiltration: The infiltration is decreased by 50% relative to the reference case.

2.5 Results

The position of the water table – defined here as the isosurface for 90% liquid saturation – for the reference case at 2 years is shown in Figure 2-5. Pressure at the repository horizon is shown on the same figure as a color map with light colors corresponding to atmospheric pressure and dark colors corresponding to high pressure. After 2 years, the water table is drawn down nearly to the repository horizon. Pressure is close to atmospheric within the repository footprint, and increases sharply away with distance from the repository outside the outermost tunnel. Positions of the 90% contours at different times are shown in the radius-depth space in Figure 2-6.

Contours of different 99%, 90%, 70%, 50% and 30% liquid saturations are shown in the radius-depth space in Figure 2-7 for three different times. Vertical profiles of saturation at the repository center and repository edge are shown in Figure 2-8 for several values of time. The 99% saturation contour has already been drawn down to the repository horizon at 1 year, but there is a significant amount of water in the unsaturated zone above that contour. For example, the 70% contour is not much different from its original position at 1 year. At 10 years, the 70% contour has also been drawn down to the repository level. The drawdown is relatively stable at that point and changes little between 10 years and 50 years. Note that the outer two tunnels (radii of 315 and 360 m) are still below the water table at 50 years. This is a consequence of radial inflow from outside the repository footprint.

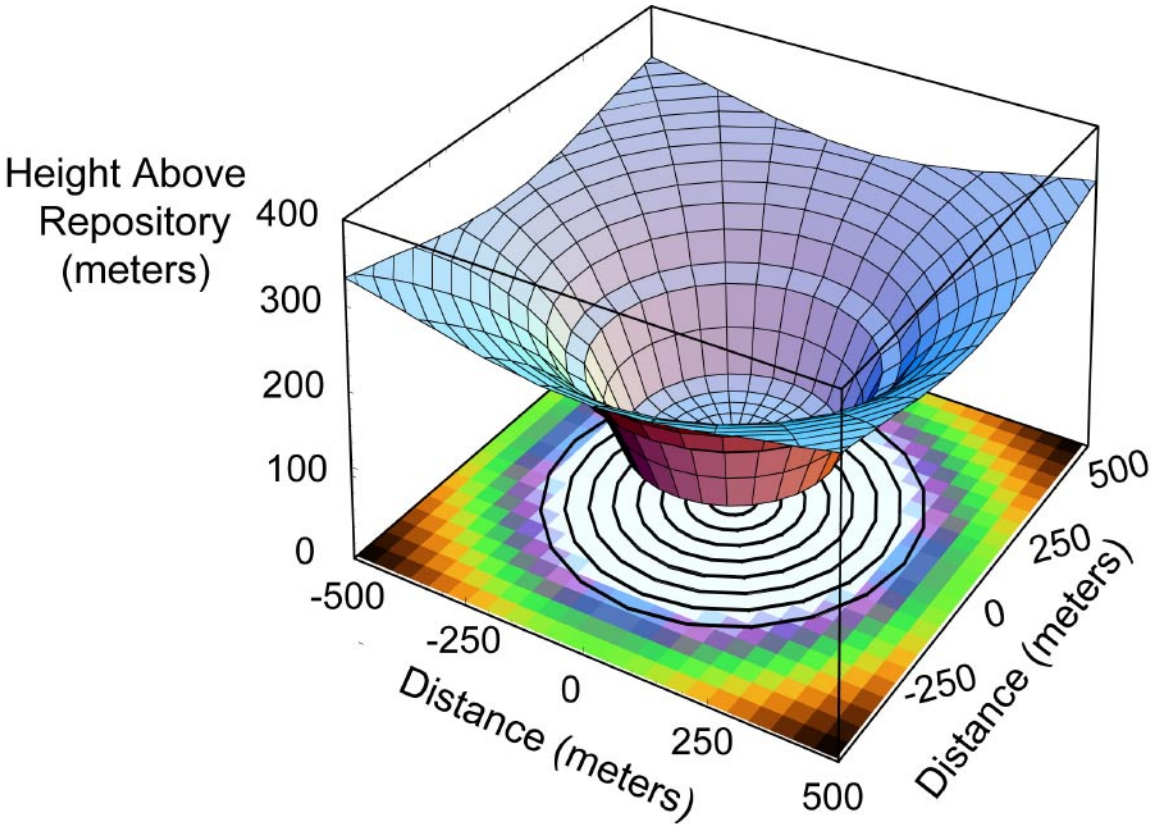

Figure 2-5. *Water table position after two years in the reference case simulation.*

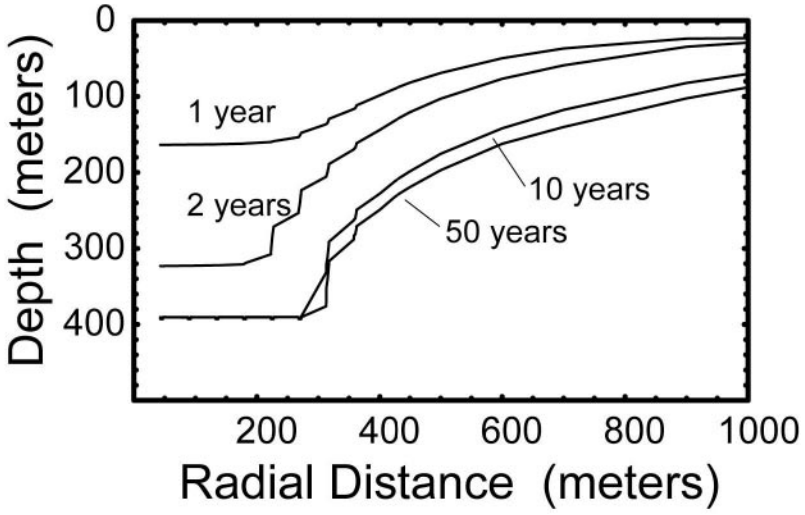

Figure 2-6. *Water table position at four different times in the reference case simulation. The tunnels are located at radii of 45, 90, 135, 180, 225, 270, 315, and 360 m.*

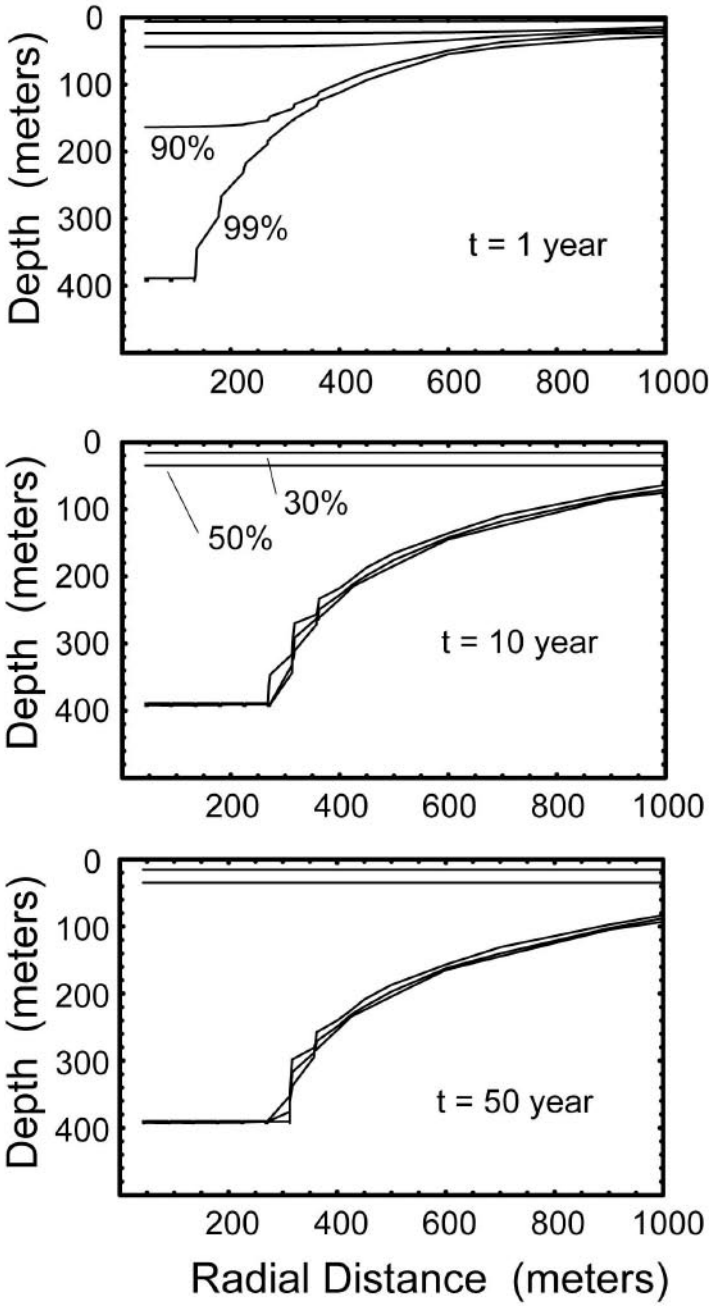

Figure 2-7. *Contours of 30, 50, 70, 90 and 99% liquid saturation at three times for the reference case simulation. The tunnels are located at radii of 45, 90, 135, 180, 225, 270, 315, and 360 m.*

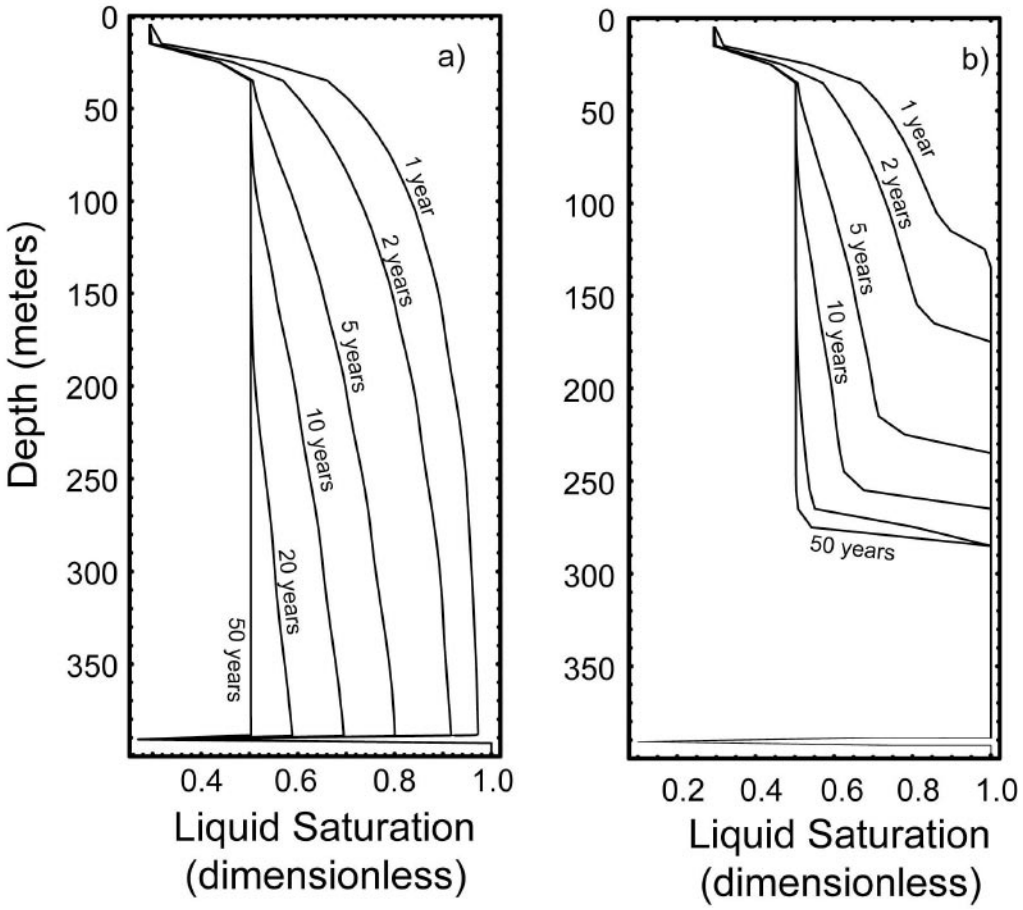

Figure 2-8. *Vertical profiles of liquid saturation at the repository center (a) and edge (b) at different times. The abrupt drop in saturation at a depth of 390 m reflects the formation of a two-phase flow region near the repository tunnels. The two-phase region has no significant effect on far-field flow.*

The saturation in the unsaturated zone depends on the infiltration rate, the absolute permeability, and the assumed characteristic curve, and remains significant throughout the simulation: about 30% near the land surface and 50% a few meters below that. Assuming a saturation value of 50% as representative, and using the 25 mm/year infiltration rate and the assumed porosity of 0.02, the downward pore velocity above the repository center is estimated at 2.5 m/year. This corresponds to a 160 year travel time from the land surface to the repository horizon at 400 m depth. That is, it takes approximately 160 years to flush or "turnover" one formation volume of water. This value for the turnover time should be regarded as a rough estimate, however, because of large uncertainties in the moisture retention curve for the fractured rock mass. The turnover time is larger for locations away from the repository center, partly due to the longer travel path to reach the repository, and partly due to the higher saturation at those locations.

Water inflows (water volume per unit time per meter of tunnel) into tunnels 1, 6 and 8 are shown in Figure 2-9. Inflows decrease quickly as the water table is drawn down, and approach a steady value after 5–10 years. This steady-state value represents water inflows from the bottom and sides of the tunnels for tunnels 1 and 6. Inflow into tunnel 8 is much greater because of edge effects.

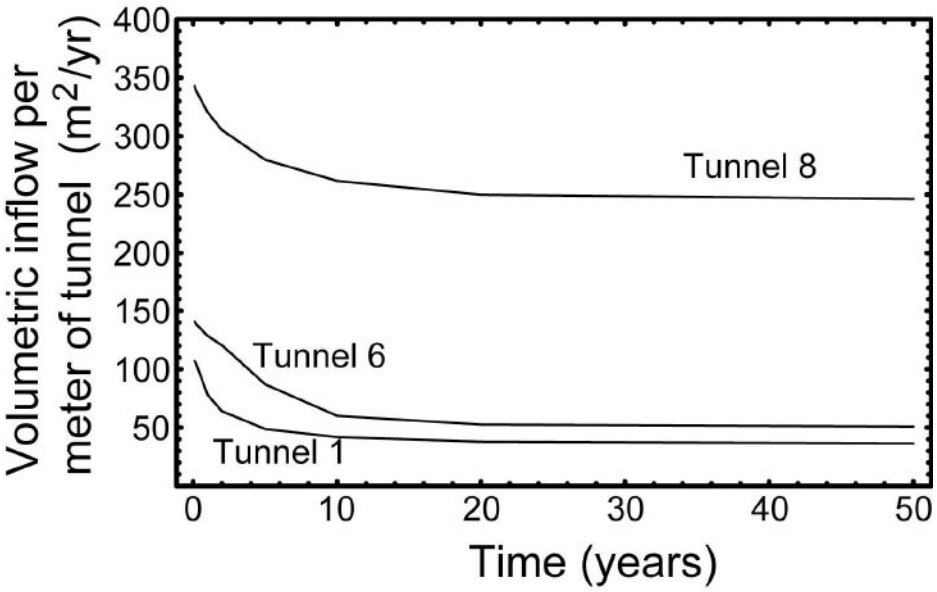

Figure 2-9. *Inflows into three tunnels as a function of time for the reference case simulation.*

At 100 years, the imposed pressure condition at the repository tunnels was removed and the water table allowed to rebound toward its original position. After about 10 years the water table returned to its original position and little effect of the repository operation was seen.

Water inflow into tunnel 6 for the unconfined aquifer simulation is compared to the reference case in Figure 2-10. Inflow for the unconfined aquifer case decreases nearly linearly with time until the steady-state value is reached, whereas inflow for the reference case decreases nonlinearly. Inflow for the unconfined aquifer simulation is nearly the same as the reference case at the start of the simulation and after 20 years, but exceeds the reference case inflows by about 70% at 10 years. Thus, the maximum error introduced by using an unconfined aquifer (free surface) code would be to predict inflows that are too large by about 70%, but for most times the error introduced is much smaller.

Inflows and water table position for the weak suction, strong suction, drain and air simulations are very close to that of the reference case. Two-phase flow in the vicinity of the tunnels is unimportant and can be neglected without introducing any significant error.

Water table position for the smeared repository simulation was nearly the same as the reference case, indicating that the global inflows are very similar. This result is similar to that of /Jacquet and Siegel, 2004/, and suggests that explicit discretization of tunnels is not necessary.

Inflows for the increased infiltration and decreased infiltration cases are very close to those of the reference case. At early times inflows are determined primarily by draining of the in-place water, while at late times the inflows are governed primarily by radial inflow into the repository footprint, hence the insensitivity to assumed infiltration rate. The saturation above the repository does depend on the infiltration rate (Figure 2-11), but not sensitively. For example, the factor of four change in infiltration when going from the decreased infiltration case to the increased infiltration case changes the saturation near the surface from about 25% to about 35%.

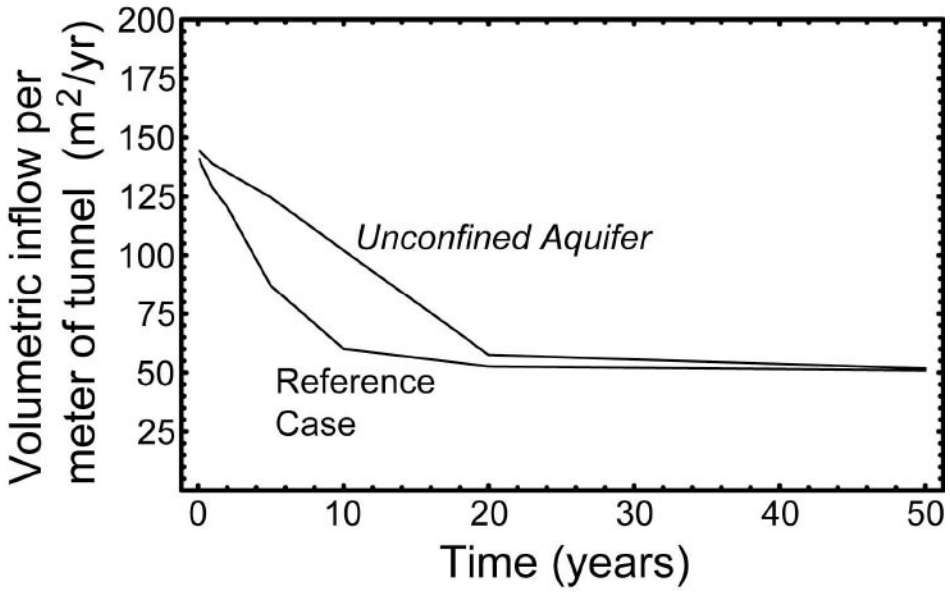

Figure 2-10. *Inflows into tunnel 6 for the Reference Case and the Unconfined Aquifer simulations.*

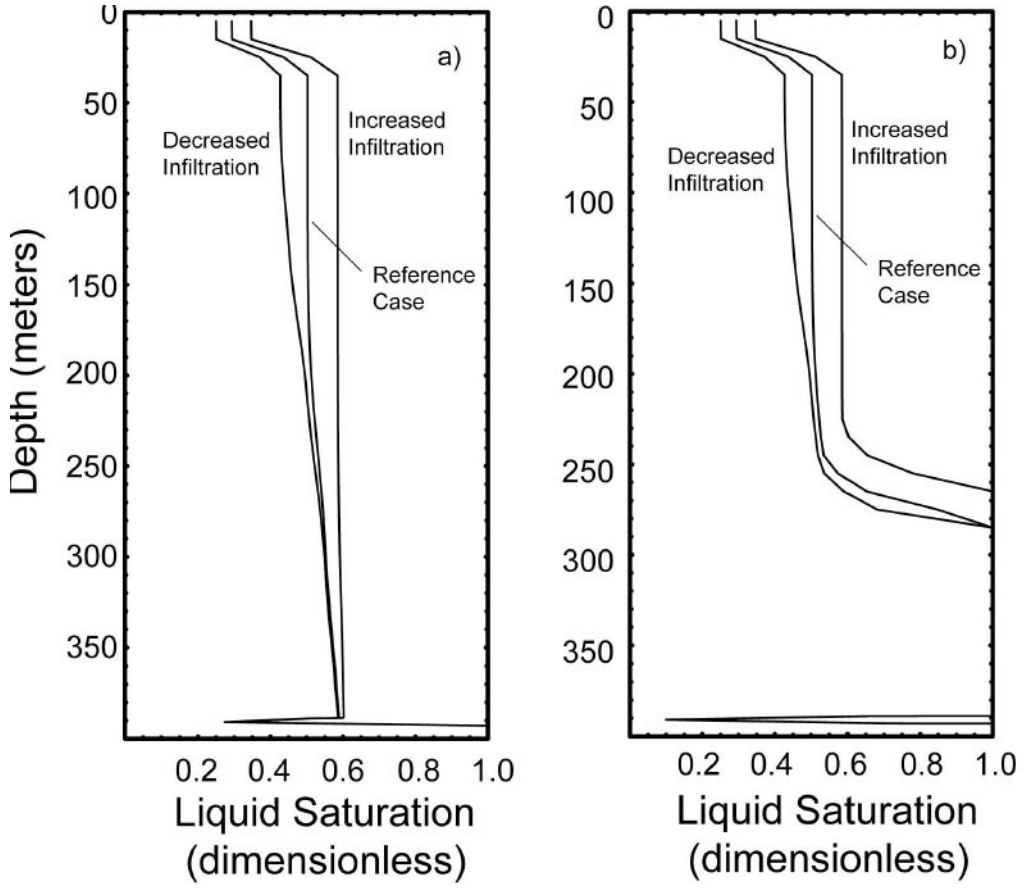

Figure 2-11. *Liquid saturation versus depth at 20 years at the repository center (a) and edge (b). Results are shown for the reference case, the increased infiltration case, and the decreased infiltration case.*

Inflows are more sensitive to the permeability. At early times there is a very nearly linear relationship between permeability and inflows. Once the system approaches a steady state, the relationship between permeability and inflow is weaker than linear, but still significant. For example, a 100% increase in permeability (reference case to the increased permeability case) results in an 87% increase in inflow into tunnel 1 at 20 years. A 50% decrease in permeability (decreased permeability case) results in a 41% decrease in inflow into tunnel 1 at 20 years. Vertical profiles of saturation at 2 years for the increased permeability, decreased permeability and reference case are shown in Figure 2-12.

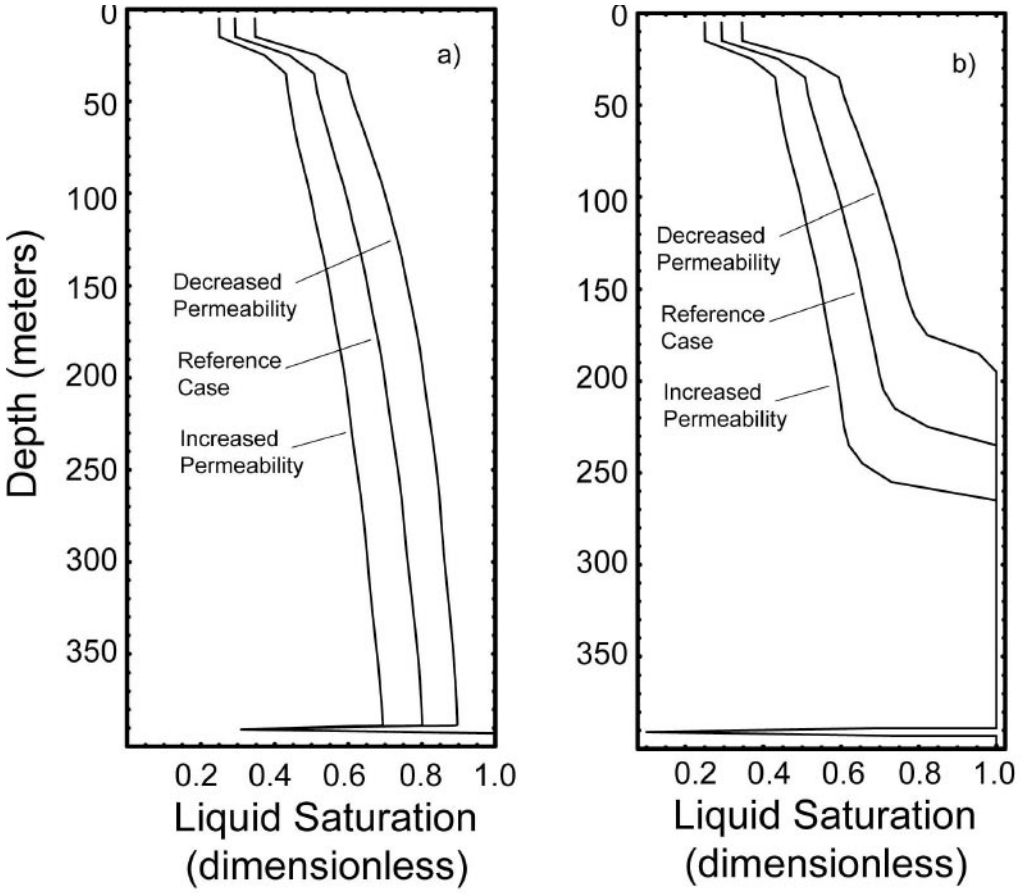

Figure 2-12. *Liquid saturation versus depth at 5 years at the repository center (a) and edge (b). Results are shown for the reference case, the increased permeability case, and the decreased permeability case.*

3 Upconing of saline water

The results in the previous section suggest that the repository can be modeled as a disk (cylindrical coordinates), with Richards equation to represent the flow dynamics. A preliminary estimate of salt concentration at the repository horizon was made using this representation. The finite-element code FEFLOW /Diersch, 2002/ was used in the assessment. FEFLOW solves Richards equation for flow plus a conservation equation for a single dissolved chemical component.

The model domain and the initial and boundary conditions for flow were identical to those in Section 2. Salt concentration was set at zero for depths of 0–500 m. The initial salt concentration varied linearly from 0 at 500 m depth to 6.5% salinity at the bottom of the modeled region. Salt concentration on the outer boundary was held fixed at this initial condition. The condition of no diffusive flux was imposed for the repository.

Salinity at 20 years is shown in Figure 3-1. The maximum salinity at the repository is about 0.7%.

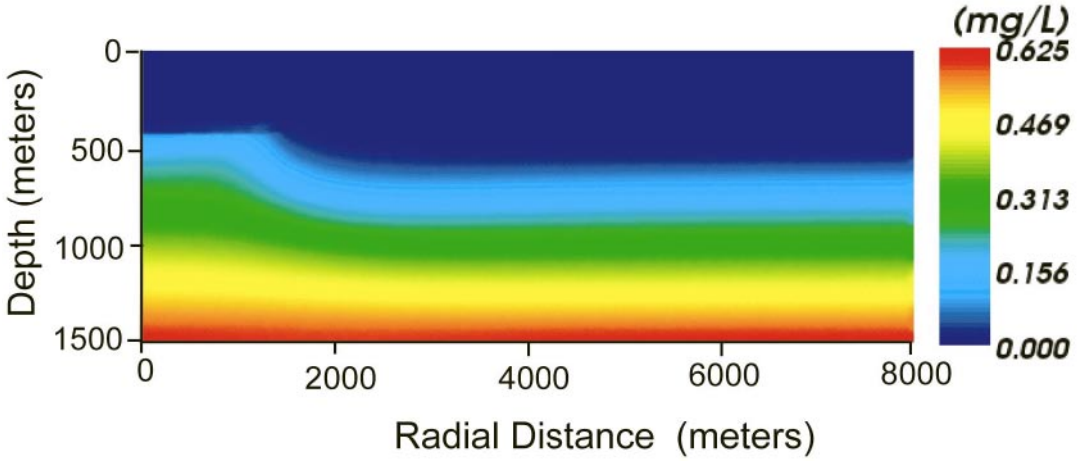

Figure 3-1. *Salt concentration at 20 years.*

4 Conclusions and recommendations

The following conclusions can be drawn from the results of the simulations:

1. Two-phase flow may be induced in the vicinity of repository tunnels during repository pre-closure operations, but the formation of a two-phase flow region will not significantly affect far-field flow or inflows into tunnels.
2. The water table will be drawn down to the repository horizon and tunnel inflows will reach a steady-state value within about 5 years.
3. Steady-state inflows at the repository edge are estimated to be about 250 m^3/year per meter of tunnel. Inflows will be greater during the transient de-watering period and less for tunnel locations closer to the repository center.
4. Significant amounts of water (50% water saturation) will remain in the unsaturated zone during repository operations.
5. If unsaturated zone processes are neglected and an unconfined aquifer (free-surface) model used, tunnel inflows will be over-predicted by as much as 70% during the dewatering phase. However, the maximum inflows and the steady-state inflows can be predicted accurately with a free-surface code.
6. The turnover time for water in the unsaturated zone is estimated to be 117 years, based on a water saturation of 50%. The estimated turnover time is inversely proportional to water content, which depends in turn on infiltration rate, absolute permeability, and the relative permeability curve.
7. Far-field flows and globally averaged inflows can be accurately calculated by considering the repository to be a disk or slab without representing individual tunnels.
8. Maximum salinity at the repository is estimated to be about 0.7%.

It should be noted that several idealizations and approximations were employed in this modeling study. Such simplifications are appropriate given the objectives of the study, and are not expected to affect the main conclusions about the consequences of different representations for open tunnels. However, the calculated values for inflows, salinity, saturation, and turnover time are dependent on the assumed values for some of the input parameters, and should be considered rough estimates only.

It is recommended that a free-surface groundwater flow model be used in future studies if the primary quantities of interest are steady-state inflows, peak inflows, or approximate water table positions. Modeling software based on Richards equation is recommended if transient inflows during the de-watering phase or unsaturated zone dynamics are also of interest.

Detailed representations of the repository tunnel layout do not appear to be necessary to obtain accurate far-field dynamics; a slab or disk representation for the repository is recommended for simplicity. However, if highly accurate estimates of peak inflows are of interestc – for sizing pumping equipment, for example – then representations of repository access shafts in three dimensions may be needed. The finite time required to construct the repository tunnels is likely to affect the peak inflows and may also need to be included. Detailed representation of shaft geometry and time-dependent boundary conditions caused by repository construction are feasible using commercial software such as FEFLOW /Diersch, 2002/.

If accurate estimates of saturation or turnover time in the upper aquifer are required, then site-specific characterization of the near-surface region is needed. For example, the saturation near the surface is likely to be affected by the presence of a soil layer, which was neglected in this study. Relative permeability curves valid at typical grid-block scales would also be needed. Experiments designed to better constrain the block-scale relative permeability curves are recommended in this situation.

This work was focused on the effects of repository operations on far-field flow. To model near-field flow in and around repository tunnels, more detailed representations of the tunnel geometries and near-field processes would be required. Simulations of backfill and buffer resaturation require the geometrical details of the tunnel and emplacement hole be represented in detail. Given that tunnel inflows will be located at discrete locations corresponding to intersecting fractures and not uniformly distributed along the tunnel, three-dimensional simulations with unstructured grids will be required. Pressure boundary conditions at the inflow locations could easily be extracted from far-field simulations like those presented here. Resaturation of backfill and buffer material is driven by pressure gradients and capillary suction of the partially saturated backfill/buffer. These driving forces are represented in Richards-equation based model. Processes that oppose the resaturation and act to slow it include air entrapment and thermal processes. These processes are not included in a Richards model. However, air entrapment is not expected to cause a significant delay in resaturation because fractures intersecting the tunnels near the tunnel crown will allow the entrapped air to escape. Similarly, thermal effects caused by the initially elevated temperatures of waste canisters relative to the surrounding material are not expected to be significant because of the large inflow rates involved, which would likely overwhelm any thermally-driven evaporation.

It is possible that thermal buoyancy-driven flow could be established in the fracture network near emplacement holes. Such flow has the potential to increase contaminant migration in the near field. Given the importance of the first few fractures to the total retention in the geosphere (i.e. Figure 5-11 of /Hartley et al. 2004/), an increase in flow around waste canisters has potential to affect total retention. To evaluate this potential thermal effect, simulations using a non-isothermal code would be required.

References

Diersch H-J G, 2002. FEFLOW – Reference Manual. WASY Ltd.

Harbaugh A W, Banta E R, Hill M C, McDonald M G, 2000. MODFLOW-2000, the U.S. Geological Survey modular ground-water model – User guide to modularization concepts and the ground-water flow process. U.S. Geological Survey Open-File Report 00-92, Denver, Colorado.

Hartley L, Cox I, Holton D, Hunter F, Joyce S, Gylling B, Lindgren M, 2004. Groundwater flow and radionuclide transport modelling using CONNECTFLOW in support of the SR Can assessment, SKB R-04-61, Svensk Kärnbränslehantering AB.

International Formulation Committee, 1967. A formulation of the Thermodynamical Properties of Ordinary Water Substance. Dusseldorf, Germany, IFC Secretariat.

Jarsjö J G, Destouni G, Gale J, 2001. Groundwater degassing and two-phase flow in fractured rock, SKB TR-01-13, Svensk Kärnbränslehantering AB.

Jaquet O, Siegel P, 2004. Local-scale modelling of density-driven flow for the phases of repository operation and post-closure at Beberg, SKB R-04-46, Svensk Kärnbränslehantering AB.

Painter S, Seth M, 2003. MULTIFLO user's manual: Two-phase nonisothermal coupled thermal-hydrological-chemical flow simulator, Center for Nuclear Waste Regulatory Analyses, Southwest Research Institute, San Antonio, Texas.

Siegel P, Jaquet O, Croise P, Bernabderrahmane H, 2002. Three-dimensional simulation of the desaturation and resaturation of a hypothetical repository concept for a deep clay formation: Assessment of key parameters, Proceedings of the Sixth International Workshop on Design and Construction of Final Repositories. Brussels, Belgium. 11–13 March, 2002.

van Genuchten M T, 1980. A closed-form equation for predicting the hydraulic conductivity of unsaturated soils. Soil Science Society of America Journal, Vol 44, Pages 892–898.

Walker D, Rhen I, Gurban I, 1997. Summary of hydrogeologic conditions at Aberg, Beberg and Ceberg, SKB TR-97-23, Svensk Kärnbränslehantering AB.